KNO SCALING IN HADRON-HADRON COLLISIONS*

By Ina Sarcevic

Theoretical Division, T-8, MS B285, Los Alamos National Laboratory, Los Alamos, New Mexico 87544, USA

(Received September 14, 1987)

We review the experimental status on KNO scaling and its violations in proton-antiproton collisions. We especially emphasize the possible solution to this problem in the parton branching model. In this model there is a new non-scaling law for the probability distribution P_{mn} of m quarks and n gluons. For very high energies, we can neglect quark evolution and find the *exact analytic* solution for the observables such as multiplicities, probability distribution and multiplicity moments. We fit the experimental data remarkably well with the assumption that initial number of gluons n_0 increases slowly with energy while the initial number of quarks m_0 decreases slowly with energy. Exciting theoretical predictions for the Tevatron Collider energies are presented.

PACS numbers: 13.85.Hd, 12.50.Ch, 12.50.Fk

1. Introduction

Most recently we have witnessed considerable renewal of interest in multiparticle production in hadron-hadron collisions, in particular KNO scaling and its violations [1]. In this lecture I will review theoretical background, experimental data, discuss theoretical models and finally present the possible solution to this problem in the context of parton branching model.

The first theoretical contribution to this problem came more than a decade ago, when Koba, Nielsen and Olesen [2] predicted a scaling law for the probability distribution

$$P_n\bar{n} = \Psi\left(\frac{n}{\bar{n}}\right), \tag{1.1}$$

where P_n is the probability distribution of getting n particles with mean multiplicity $\bar{n}$ and $\Psi\left(\frac{n}{\bar{n}}\right)$ is energy independent function. Their prediction was based on assumption of validity

* Presented at the XXVII Cracow School of Theoretical Physics, Zakopane, Poland, June 3–15, 1987.

of Feynman scaling for the many particle inclusive cross section. Namely, if we consider k particles produced in hadron-hadron collision with $p_1 \dots p_k$ momenta, the normalized inclusive cross section $\phi^{(k)}(p_1 \dots p_k; s)$ defined as

$$\phi^{(k)}(p_1 \dots p_k; s) = \frac{1}{\sigma} \frac{d^{3k}\sigma_{\text{incl}} \sqrt{p_1^2+m_1^2} \dots \sqrt{p_k^2+m_k^2}}{d^3 p_1 \dots d^2 p_k} \tag{1.2}$$

is a function of $p_\perp$, Feynman variable $x = \dfrac{2p_\parallel}{\sqrt{s}}$ and the center of energy $\sqrt{s}$. The assumption that Feynman scaling is valid for this cross section implies that $\phi^{(k)}(x_1 \dots x_k, p_{1\perp} \dots p_{k\perp})$ is energy independent function. Multiplicities can be obtained from the inclusive cross section by integrating $\phi^{(1)}(p_1, s)$ over the momentum p_1

$$\bar{n} = \int \frac{d^3 p_1}{\sqrt{p_1^2+m_1^2}} \phi^{(1)}(p_1, s). \tag{1.3}$$

The multiplicity moments defined as

$$K_k = \frac{\overline{n(n-1) \dots (n-k+1)}}{\bar{n}^k} \tag{1.4}$$

can be obtained by integrating $\phi^{(k)}$ over the momenta $p_1 \dots p_k$.

Therefore the assumption of Feynman scaling for $\phi^{(k)}$ implies that $\bar{n}$ grows logarithmically with energy while the moments K_m are energy independent. This can be seen if we rewrite the multiplicities as

$$\bar{n} = \int_{-Y}^{Y} dy \bar{\phi}^{(1)}(y, s), \tag{1.5}$$

where

$$y = \tfrac{1}{2} \ln \frac{\sqrt{s}+p_\perp}{\sqrt{s}-p_\perp} \tag{1.6}$$

and

$$\bar{\phi}^{(1)}(y, s) = \int dp_{1\perp} \phi^{(1)}(p_1, s). \tag{1.7}$$

Clearly the maximum rapidity is related to the energy by the simple relationship

$$Y = \tfrac{1}{2} \ln \left(\frac{s}{m_p^2} \right). \tag{1.8}$$

Assuming the validity of Feynman scaling ($\bar{\phi}^{(1)}(y, s)$ is energy independent) and taking the limit when $s \to \infty$, we get

$$\bar{n} \to \bar{\phi}^{(1)}(0) \ln s \tag{1.9}$$

and

$$\overline{n(n-1) \dots (n-k+1)} \to \bar{\phi}^{(1)}(0) (\ln s)^k. \tag{1.10}$$

Therefore the multiplicity moments K_k defined by Eq. (1.4) are energy independent. We also note that KNO scaling also implies that moments defined as

$$C_q = \frac{\overline{n^q}}{\bar{n}^q} \tag{1.11}$$

are energy independent.

2. Experimental data

At that time when KNO scaling was proposed the available energy was $10\ \text{GeV} \leqslant \sqrt{s} \leqslant 30\ \text{GeV}$ and it was hard to test this prediction in this small energy range. Going from the Fermilab energies $\sqrt{s} \sim 10\ \text{GeV}$ up to ISR energies $\sqrt{s} \sim 30\ \text{GeV}$ [3] it looked as the scaling has already been reached. However the most recent data from $Sp\bar{p}S$ Collider ($200\ \text{GeV} \leqslant \sqrt{s} \leqslant 900\ \text{GeV}$) show dramatic scaling violations [4]. In Figs 1–3 we see that KNO scaling violations observed by the UA5 Group which are manifested in widening of the probability distribution, increase of the multiplicity moments C_q and the violation of the logarithmic growth of the multiplicities. From Fig. 2 we notice that KNO scaling violation is more apparent in the case of higher moments.

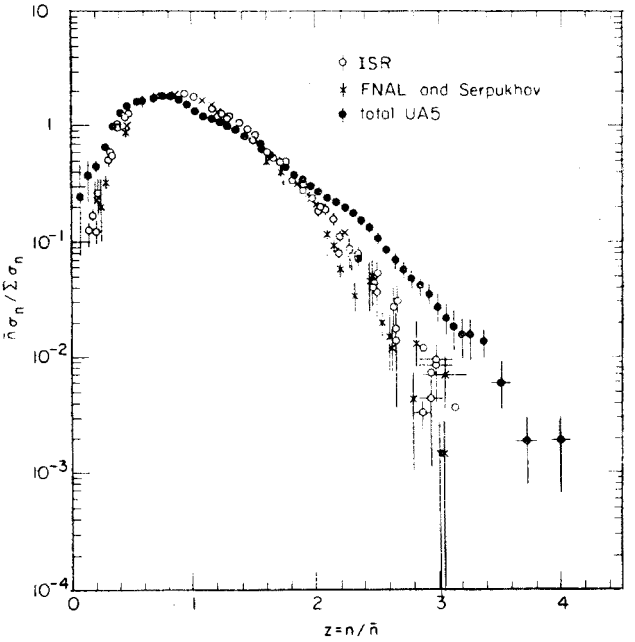

Fig. 1. The multiplicity distributions $\bar{n}\dfrac{\sigma_n}{\Sigma\sigma_n}$ plotted as a function of $z = \dfrac{n}{\bar{n}}$ for the energy range from FNAL ($\sqrt{s} \sim 10\ \text{GeV}$) through ISR ($\sqrt{s} \sim 63\ \text{GeV}$) to CERN $Sp\bar{p}S$ Collider ($\sqrt{s} \sim 540\ \text{GeV}$), Ref. [4]

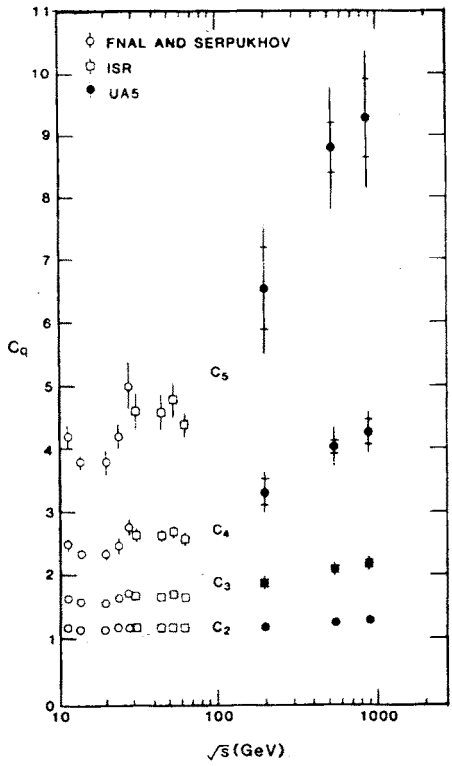

Fig. 2. From Ref. [7], the multiplicity moments C_q ($q = 2...5$) plotted for FNAL, ISR and Sp$\bar{p}$S energies

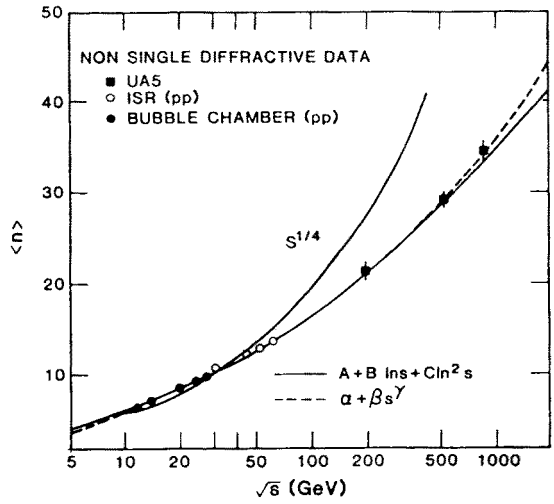

Fig. 3. The energy dependence of the mean multiplicity in energy range 10 GeV $\leqslant \sqrt{s} \leqslant$ 900 GeV fitted with the curves of the form $s^{1/4}$, $A+B\ln s+C\ln^2 s$ and $\alpha+\beta s^{\gamma}$. The values for A, B and C, α, β and γ are given below Eq. (3.31)

The UA5 group also fitted their data with the negative binomial distribution [5]

$$P_n^k(\bar{n}) = \frac{(n+k-1)!}{n!(k-1)!}(\bar{n}/k)^k(1+\bar{n}/k)^{-n-k}, \tag{2.1}$$

with two parameters $\bar{n}$ and k. In the energy range 10 GeV $\leqslant \sqrt{s} \leqslant$ 900 GeV they found that the best fit is with parameter k decreasing from 20 to 3. This distribution was proposed in many different theoretical models [6], but without clear understanding of the behavior of the parameter k. Another interesting observation is that the probability distribution has different shape for different rapidity regions, namely it is much narrower for the full rapidity range ($y < 5$) than for the central region ($y < 1.5$) [7]. This can be seen in Fig. 4.

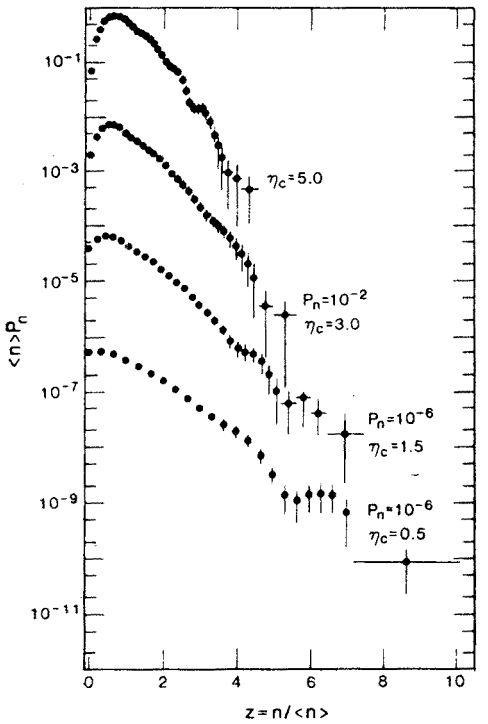

Fig. 4. From Ref. [7], the $\bar{n}P_n$ plotted versus $z = \frac{n}{\bar{n}}$ for different rapidity regions. As the rapidity increases the function $\bar{n}P_n$ becomes wider

Recently, the UA1 group found out that the fraction of events containing at least one jet with $E_t > 5$ GeV (so called "mini-jets") is increasing with energy [8]. For the $S\bar{p}pS$ Collider energies it increases from 5% to 17%. This gives a new hope for the QCD based models. It also means that it is important to consider carefully different cuts in p_t and the fractional momenta x.

3. Theoretical models

3.1. Dual parton model

This model [9] is based on the assumption that the interaction between two hadrons after the collision separates each hadron into two colored systems: quark and diquark. The chains are formed from quark-and diquark of different hadrons. Each chain corresponds to two back-to-back jets in its center of mass frame. In this picture, gluons mediate the interactions, "dress" the quarks and produce $q\bar{q}$ pairs. In this model the KNO scaling violations are due to the increase of the rescattering component of the inelastic collision. This component is coming from the multiple inelastic collisions and it corresponds to the creation of the multichains. Most recently, new semi-hard component has been added to this model. This component corresponds to the observed "mini-jets" [10].

3.2. Geometrical models

In these models the KNO scaling is directly related to the geometrical scaling. Geometrical scaling relates in a specific way the elastic differential cross section to the imaginary and real parts of the scattering amplitude. In these models at very high energies the hadronic elastic amplitude is decomposed into a part which is energy dependent and the part which is a function of the high energy scaling variable $\tau = -t\sigma_{tot}(s)$, where t is the four-momentum transfer. This implies that differential cross section scales with the variable τ and σ_{el}/σ_{tot} is energy independent. This prediction was found to be violated at the CERN collider energies.

Yang and Chou [11] proposed an improved geometrical model in which the probability distribution for the multiparticle production in hadron-hadron collision is the superposition of many Poisson distributions each characterized with a different impact parameter b. As the energy increases the impact parameter increases and the process becomes more stochastic. This prediction can be expressed in terms of forward-backward multiplicity distribution which will be represented with the straight line at very high energies.

This model is also applied to e^+e^- collisions in which case $b = 0$ and the probability distribution is composed of two Poisson distributions [12].

In the three-fireball model [13] target, projectile and central region are formed after the collision each producing n_i particles (i = t, p, c). The KNO scaling violations in this model are due to different energy dependence of the mean multiplicity of each region. Another adequate explanation is that the violations are due to the increase of the size of the central fireball relative to the sizes of the other fireballs. The KNO scaling function in this model has the following form

$$\psi(z_i) \sim z_i^{k-1} e^{-kz_i}. \tag{3.1}$$

At low energies it is found that $k = 6$ while at high energies $k = 2$.

3.3. Models with QCD framework

In the cluster model [4] hadrons are produced in two steps: first a far off shell quark radiates gluons which form clusters, then these clusters turn into particles. The scaling violation comes from the energy dependence of the number of clusters as well as the energy

dependence of the number of particle per cluster. However this model predicts the slow narrowing of the distribution which is in contradiction with the experimental data.

In the soft gluon bremsstrahlung model [15] the violations are due to the three-gluon coupling which becomes the dominant process at collider energies. The multiplicities also have contributions from quark bremsstrahlung as well as from the soft gluon bremsstrahlung. The ratio of these two processes is an energy dependent parameter. In the quark--parton model [16] multiplicities have a contribution from quark-quark collision as well as gluon-gluon collision. The scaling violations observed at Collider energies are due to the rising component of the gluon-gluon collisions. Multiplicities are given by

$$\bar{n} = \bar{n}_q \frac{\sigma_q}{\sigma_{incl}(s)} + \bar{n}_g \frac{\sigma_g(s)}{\sigma_{incl}(s)}, \tag{3.2}$$

where σ_q is the constant part of the total cross section while σ_g is the energy dependent ($\sigma_g \sim \ln^2 s$) introduced on a phenomenological grounds. This model can be applied to both non-single diffractive as well as the inclusive data. The probability distributions are obtained with a cutoff in the momenta ($x = 0.03$) because of the divergence of the parton distributions at $x = 0$. The available experimental data are very poor in the region when $x < 0.1$ especially at low Q, and indeed there is no firm theoretical understanding of the gluon distributions in this region.

Finally, the QCD jet models will be discussed in Sect. 4 in relation to our branching model.

3.4. Stochastic models

In these models scaling is related to the general statistical and dynamical properties of the multiparticle production. The probability distribution proposed by Carruthers and Shih [6] is the negative binomial distribution

$$P_n^k(\bar{n}) = \frac{(n+k-1)!}{n!(k-1)!} \left(\frac{k}{\bar{n}}\right)^k \left(1+\frac{k}{\bar{n}}\right)^{-n-k} \tag{3.3}$$

which corresponds to k sources (clusters) emitting fields behaving as gaussian random variables. The sources have equal strength with average multiplicity $\bar{n}/k$. In the large n and $\bar{n}$ limit $\bar{n}P_n^k(\bar{n})$ approaches the scaling function:

$$\bar{n}P_n \to \psi\left(z = \frac{n}{\bar{n}}\right) = \frac{k^k}{(k-1)!} e^{-kz} z^{k-1}. \tag{3.4}$$

It is easy to see that the negative binomial distribution is the Poisson transform of $\psi(z)$:

$$P_n(\bar{n}) = \int \frac{(z\bar{n})^n}{n!} e^{-\bar{n}z} \phi(z). \tag{3.5}$$

The origin of the Poisson transform can be seen by looking at the density matrix formalism [17]. Namely, the probability distribution can be expressed as a diagonal element of the

density matrix

$$P_n = \langle n|\varrho|n\rangle, \tag{3.6}$$

where ϱ is the density matrix given by

$$\varrho = \int \frac{d^2\alpha}{2\pi}\, \phi(\alpha)\, |\alpha\rangle\, \langle\alpha|. \tag{3.7}$$

The coherent states $|\alpha\rangle$ are defined as:

$$|\alpha\rangle = e^{-|\alpha|^2} \int_{n=0}^{\infty} \frac{\alpha^n}{\sqrt{n!}} |n\rangle. \tag{3.8}$$

The function $\phi(\alpha)$ is a dynamical weight function. If we identify $\psi(z)$ as:

$$\psi(z) = \frac{\bar{n}}{2\pi} \int \frac{d\phi}{2\pi}\, \Phi(\alpha = e^{i\phi}\sqrt{z\bar{n}}) \tag{3.9}$$

then the probability distribution is just the Poisson transform of $\psi(z)$. As an example, let us consider the following single weight functions:

$$\begin{aligned} \phi_1(\alpha) &= \delta(\alpha-\beta), \\ \phi_2(\alpha) &= \frac{e^{-|\alpha|^2/N}}{\pi N}, \\ \phi_3(\alpha) &= \frac{e^{-|\alpha-\beta|^2/N}}{\pi N}. \end{aligned} \tag{3.10}$$

The corresponding probability distributions are [18]:

$$\begin{aligned} P_n &= \frac{1}{n!}\, |\beta|^{2n} e^{-|\beta|^2}, \qquad P_n = \frac{N^n}{(1+N)^{n+1}}, \\ P_n &= \frac{N^n}{(1+N)^{n+1}}\, e^{-\frac{|\beta|^2}{1+N}} L_n\left(-\frac{|\beta|^2}{N(1+N)}\right). \end{aligned} \tag{3.11}$$

In the case of k oscillators of equal strength each having the same weight function

$$\phi_i = e^{-|\alpha_i-\beta|^2/N} \tag{3.12}$$

the probability distribution is:

$$P_n^k(N, |\beta|^2) = \frac{\left(\frac{N}{k}\right)^n}{\left(1+\frac{N}{k}\right)^{n+k}}\, e^{\frac{-|\beta|^2}{1+\frac{N}{k}}} L_n^{(k-1)}\left(\frac{-k|\beta|^2/N}{1+N/k}\right), \tag{3.13}$$

with the corresponding multiplicity

$$\bar{n} = N + |\beta|^2. \tag{3.14}$$

The probability $P_n^k(N, |\beta|^2)$ given by Eq. (3.13) is sometimes referred to as a Glauber--Lachs formula. In the stochastic picture proposed by Carruthers et al. [6] the parameters $|\beta|^2$ and N are coherence and incoherence respectively. In the limit when $|\beta|^2 \to 0$ the probability distribution becomes the negative binomial distribution, while for the case where $N \to 0$ and $k = 1$ it is the Poisson distribution. The fact that the ratio of N and $|\beta|^2$ changes the shape of the distribution in the way described above has been used to explain the widening of the distribution as the increase of the incoherence (noise) with energy in the hadron--hadron collisions. The Glauber-Lachs probability distribution is used as an alternative for the negative binomial distribution even though the number of stochastic models with the negative binomial distribution as their prediction has enormously increased in the last year as a consequence of the remarkably good fit to the experimental data done by the UA5 Group [5]. However there is still no understanding of the behavior of the parameter k which, according to the fits, decreases with energy. In the model of Giovannini and Van Hove [19] k is the ratio of cascading and partial stimulated emission and it is rapidity dependent. However the dynamics is missing and k is just a parameter fitted to the data. They do not obtain the energy dependence of k. An alternative model is a statistical model based on

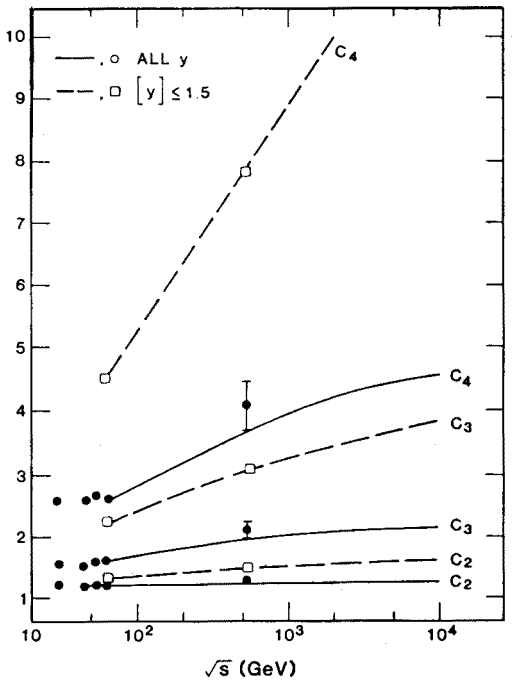

Fig. 5. From Ref. [7], the multiplicity moments C_q ($q = 2 \ldots 5$) plotted versus energy for the total rapidity region and for $|y| < 1.5$. The scaling violations are more expressed for the restricted rapidity region than for the whole rapidity region

analogy with the Feynman-Wilson "gas". In this model we have shown that the onset of KNO scaling is an indication of a phase transition [20]. We have argued that this phase transition corresponds to the transition of the hadronic matter to a quark-gluon plasma [21]. In this model the probability distribution is very similar to the negative binomial distribution (moments C_2 are the same!) and the parameter k is related to the coherence length. It is also possible to explain the rapidity dependence of the moments C_q observed by UA5 Group [4] (See Fig. 5).

3.4.1. The Fokker-Planck type evolution equations in the stochastic model

In the context of the stochastic model the multiparticle production is a stochastic--dissipative process that can be described appropriately by the time evolution equation of the Fokker-Planck type. This approach was developed by Carruthers [22]. The Fokker--Planck equation for the KNO scaling function $\psi(z, t)$ was found to be

$$\frac{\partial \psi}{\partial t}(z, t) = -\frac{\partial}{\partial z}\left[z\left(\frac{2h}{Q} - 1 - \frac{2b}{Q} z^{\gamma} - z\frac{\partial}{\partial z}\psi(z, t)\right)\right], \tag{3.15}$$

where

$$\langle f(t)f(t')\rangle = Q\delta(t-t') \tag{3.16}$$

and Q is the noise strength, $f(t)$ is a fluctuating force and b, h, γ are the parameters.

The corresponding Langevin equation is:

$$\frac{dz}{dt} = hz - bz^{1+\gamma} + zf(t). \tag{3.17}$$

This is actually the rate equation for the number populations when $f(t)$ is described by gaussian white noise. The stationary solution (long-time) of the Fokker-Planck equation is:

$$\psi(z) = Nz^{(2h/Q-1)}e^{-(2bz^{\gamma}/Q\gamma)}. \tag{3.18}$$

When $\gamma = 1$ and $k = 2b/Q = 2h/Q$ this $\psi(z)$ is the Γ distribution defined by Eq. (3.4). With a similar approach Biyajima and Suzuki [23] obtain the following Fokker-Planck equation for $\psi(z, t)$:

$$\frac{\partial \psi(z, t)}{\partial t} = -\frac{\partial}{\partial z}\left[g(z)\left(\frac{k-1}{z} - k - \frac{\partial}{\partial z}\right)\psi(z, t)\right]$$

$$= -\frac{\partial}{\partial z}\left[g(z)\left(\frac{k-1}{z} - k\right) + \frac{\partial g(z)}{\partial z}\right]\psi(z, t) + \frac{\partial^2}{\partial z^2}[g(z)\psi(z, t)], \tag{3.19}$$

where $g(z) = \lambda_0 z$.

After taking the Poisson transform of this equation we can get the evolution equation for the probability distribution:

$$\frac{\partial P_n}{\partial t} = -\lambda_0 \bar{n} n P_n - \lambda_0(\bar{n}+k) n P_n - \lambda_0 \bar{n} k P_n + \lambda_0 \bar{n}(n-1) P_{n-1}.$$

$$+\lambda_0(\bar{n}+k)(n+1)P_{n+1} + \lambda_0 \bar{n} k P_{n-1}. \tag{3.20}$$

This equation can be solved for different initial conditions. If at $t = 0$

$$P_n(t=0) = \delta_{n,0},$$

$$P_n(t=0) = \frac{(n+k-1)!}{n!(k-1)!}\left(\frac{k}{\bar{n}}\right)^k \left(1+\frac{k}{\bar{n}}\right)^{-n-k},$$

$$P_n(t=0) = (\bar{n}_0)^n \frac{e^{-\bar{n}_0}}{n!} \tag{3.21}$$

then

$$P_n(t) = \frac{\bar{n}^n e^{-n}}{n!}, \quad P_n(t) = \frac{(n+k-1)!}{n!(k-1)!}\left(\frac{k}{\bar{n}}\right)^k \left(1+\frac{k}{\bar{n}}\right)^{-n-k},$$

$$P_n(t) = \frac{\alpha^n}{(1+\alpha)^{n+k}} e^{-\frac{\bar{n}_0 e^{(A-B)t}}{1+\alpha}} L_n^{(k-1)}\left(-\frac{\bar{n}_0 e^{(A-B)t}}{\alpha(1+\alpha)}\right), \tag{3.22}$$

where $A = \lambda_0 \bar{n}$, $\tilde{A} = \lambda_0 \bar{n} k$, $B = \lambda_0(\bar{n}+k)$ and $\alpha = n/k$.

The corresponding multiplicities are

$$\bar{n} = \left[\frac{\tilde{A}}{A-B}(e^{(A-B)t}-1)\right],$$

$$\bar{n}' = \left[\frac{\tilde{A}}{A-B}(e^{(A-B)t}-1)\right]\bar{n} + e^{(A-B)t}\frac{\tilde{A}}{A-B},$$

$$\langle n \rangle = \bar{n}_0 e^{(A-B)t} + \frac{\tilde{A}}{A-B}(e^{(A-B)t}-1). \tag{3.23}$$

In the large n, $\bar{n}$ limit

$$\bar{n} P_n(z,t) = \frac{k^k}{(1-e^{(A-B)t})^k}\left(\frac{z}{e^{(A-B)t}}\right)^{\frac{k-1}{2}} e^{-k\frac{(z+e^{(A-B)t})}{[23]}} I_{k-1}\left(\frac{2k\sqrt{z e^{(A-B)t}}}{1-e^{(A-B)t}}\right)$$

$$\to \frac{k^k}{(k-1)!} z^{k-1} e^{-kz}. \tag{3.24}$$

The energy dependence of the multiplicities in all stochastic models has to be put in by hand and it is usually taken to be a simple power law

$$\bar{n} \sim s^{1/4}. \tag{3.25}$$

This power law for the multiplicity first arose in the context of the Landau hydrodynamical model and was extensively used by Carruthers and Zachariasen [24]. However this power law is probably of more general validity as it can be derived in a naive branching model of fireball decay. If we start with one "fireball" (cluster) of invariant mass w that splits into two smaller "fireballs" (clusters) with equal mass w/c then after ν steps they will reach energy w_0 and hadronize. Then the final multiplicity is

$$\bar{n} \sim 2^{\nu}, \tag{3.26}$$

where

$$\nu = \frac{1}{\ln c} \ln \frac{w}{w_0}. \tag{3.27}$$

Therefore

$$\bar{n} \sim (w/w_0)^{\ln 2/\ln c}. \tag{3.28}$$

If $c = 4$ then

$$\bar{n} \sim (w/w_0)^{1/2}. \tag{3.29}$$

We compare this power law with data in Fig. 3. We note that the multiplicity does not increase as fast as a power law. Furthermore it also rises faster than expected from the hypothesis of Feynman scaling adopted by Koba, Nielsen and Olesen ($\bar{n} \sim \ln s$). Therefore it seems reasonable to regard the power law as an upper bound and the original $\ln s$ as a lower bound. The multiplicities from 10 GeV up to 900 GeV were fitted with the following formulas:

$$\bar{n} \sim A + B \ln s + C \ln^2 s \tag{3.30}$$

and

$$\bar{n} \sim \alpha + \beta s^{\gamma}, \tag{3.31}$$

where $A = 2.7 \pm 0.7$, $B = 0.03 \pm 0.21$, $C = 0.167 \pm 0.016$, $\alpha = -7.0 \pm 1.3$, $\beta = 7.2 \pm 1.0$ and $\gamma = 0.127 \pm 0.009$. The energy dependence of the mean multiplicities in energy range $10\ \text{GeV} < \sqrt{s} < 900\ \text{GeV}$ fitted with the curves of the form $s^{1/4}$, $A + B \ln s + C \ln^2 s$ and $\alpha + \beta s^{\gamma}$.

4. The parton branching model

4.1. Introduction

In this Chapter we examine the problem of hadronic multiplicity distributions in the parton branching model [25]. Our motivation is to understand analytically how dynamics affects multiplicity. We derive the probability distribution P_{mn} of m quarks and n gluons and show that it does not obey exact KNO scaling law [25]. The violation of the scaling is due to the fact that gluons can produce quarks by converting into quark and antiquark pair and quarks can produce gluons by bremsstrahlung. We assume that the dynamics

of QCD processes comes in three steps. First there is a collision of leptons or partons which gives an initial number m_0 of quarks and n_0 of gluons. The dynamics in this step is contained in the parton distribution functions and interactions, if the colliding particles are hadrons. Second, the initial m_0 and n_0 partons (quarks q or gluons g) undergo branching, $g \to gg$, $q \to gg$, $g \to q\bar{q}$, with probabilities A, $\tilde{A}$ and B respectively. For this step, it is possible to write an evolution equation for P_{mn}, the probability of finding m quarks and n gluons, which incorporates the dynamics of the branching probabilities. In the third step the partons hadronize at energy Q_0 according to the dynamics of fragmentation functions. We focus on steps one and two, and we assume that the final number of observed hadrons is directly proportional to the final number of partons. The evolution equation of step two leads to a solution which displays KNO scaling violation. However, the initial conditions for step two arise from step one and they can also give KNO scaling violation, as we discuss in Sect. 4.2.3. Due to the increase of the activity of the gluons inside the hadrons we find that the widening of the probability distribution will stop at some asymptotic energies, which in our model corresponds to Tevatron energies [26].

4.2. QCD branching

4.2.1. The coupled quark-gluon equations

In step two, some initial numbers m_0 of quarks and n_0 of gluons produced with a probability distribution $P(m_0, n_0)$ in step one, undergo branching. We study the evolution of these partons through three branching processes with averaged probabilities at the vertices: $g \to gg$ with probability A (3-gluon vertex, gluon bremsstrahlung), $q \to qg$ with probability $\tilde{A}$ (quark bremsstrahlung) and $g \to q\bar{q}$ with probability B. These probabilities in perturbative QCD satisfy $A > \tilde{A} > B$ in any energy range. In the leading logarithmic approximation these probabilities can be obtained by integrating splitting functions

$$P_{g\to g} = \frac{2N_c}{x}, \quad P_{q\to g} = \frac{N_c^2-1}{N_c x}, \quad P_{g\to q} = \frac{N_f}{2}(x^2+(1-x)^2) \tag{4.1}$$

over the fractional momenta x. We note that $\frac{\tilde{A}}{A} = \frac{N_c^2-1}{2N_c^2}$.

Our evolution parameter t is the "natural" QCD evolution parameter

$$t = \frac{6}{11N_c - 2N_f} \ln \frac{\ln Q^2/\mu^2}{\ln Q_0^2/\mu^2}, \tag{4.2}$$

where N_c = number of colors, N_f = number of flavors, Q = parton initial invariant mass, Q_0 = hadronization energy, and μ = scale parameter of the running coupling constant.

The probability P_{mn} for m quarks and n gluons satisfies the evolution equation

$$\frac{\partial P_{mn}}{\partial t} = -AnP_{mn} - BnP_{mn} - AmP_{mn} + A(n-1)P_{mn-1} + \tilde{A}mP_{mn-1} + B(n+1)P_{m-2n+1}. \tag{4.3}$$

Assuming that P_{mn} is a smooth function of m and n using a Taylor series expansion (for large m and n) in the continuous variables m and n, we keep terms of order P and (m or n) $\partial P/\partial(m$ or $n)$ to obtain the differential equation

$$\frac{\partial P(m,n)}{\partial t} = -[A-B]P(m,n)+[-(A-B)n-\tilde{A}m]\frac{\partial P(m,n)}{\partial n} - 2Bn\frac{\partial P(m,n)}{\partial m}. \tag{4.4}$$

Since m and n are large we do not keep higher order terms. We solve Eq. (4.4) by the method of first integrals to get the form of $P(m, n, \bar{m}, \bar{n}, \bar{m}_0, \bar{n}_0)$ given below in Eq. (4.9). It simplifies notation to define

$$a_0 = A-B,$$

$$\lambda_0^{\pm} = \frac{a_0}{2}(1\pm\sqrt{1+8\tilde{A}B/a_0^2}). \tag{4.5}$$

Then the mean multiplicities m and n mix via the equations

$$\frac{d\bar{m}}{dt} = 2B\bar{n}$$

and

$$\frac{d\bar{n}}{dt} = a_0\bar{n}+\tilde{A}\bar{m}, \tag{4.6}$$

with solutions

$$\bar{m} = \frac{2B}{\sqrt{1+8\tilde{A}B/a_0^2}}\left[\left(\bar{n}_0+\frac{\tilde{A}}{\lambda_0^+}\bar{m}_0\right)e^{\lambda_0^+ t}+\frac{\lambda_0^+}{2B}\left(\bar{m}_0-\frac{2B}{\lambda_0^+}\bar{n}_0\right)e^{\lambda_0^- t}\right],$$

$$\bar{n} = \frac{1}{\sqrt{1+8\tilde{A}B/a_0^2}}\left[\lambda_0^+\left(\bar{n}_0+\frac{\tilde{A}}{\lambda_0^+}\bar{m}_0\right)e^{\lambda_0^+ t}-\tilde{A}\left(\bar{m}_0-\frac{2B}{\lambda_0^+}\bar{n}_0\right)e^{\lambda_0^- t}\right]. \tag{4.7}$$

Since $\lambda_0^+ > 0$ and $\lambda_0^- < 0$, the $e^{\lambda_0^- t}$ terms vanish for large t. Also, if gluon bremsstrahlung dominates, so that $A \gg \tilde{A}, B$, then $\lambda_0^+ \to a_0 \to A$, $\lambda_0^- \to 0$, $\sqrt{1+8\tilde{A}B/a_0^2} \to 1$, and

$$\bar{n} \to \bar{n}_0 e^{At}+\frac{\tilde{A}}{A}\bar{m}_0 e^{At}$$

and

$$\bar{m} \to \frac{2B}{A}\bar{n}+\bar{m}_0. \tag{4.8}$$

The mean number of gluons then dominates the mean number of quarks as expected. Equation (4.8) says that the contributions to $\bar{m}$ are from the initial number $\bar{m}_0$ and from pair production (B), while $\bar{n}$ comes from branching of the $\bar{n}_0$ initial gluons and quark bremsstrahlung ($\tilde{A}$) coming from $\bar{m}_0$.

The solution to Eq. (4.4) is

$$P(m, n, \bar{m}, \bar{n}, \bar{m}_0, \bar{n}_0) = \frac{\left(\bar{m}_0 - \frac{2B}{\lambda_0^+}\bar{n}_0\right)\left(\bar{n}_0 + \frac{\tilde{A}}{\lambda_0^+}\bar{m}_0\right)}{\left(\bar{m} - \frac{2B}{\lambda_0^+}\bar{n}\right)\left(\bar{n} + \frac{\tilde{A}}{\lambda_0^+}\bar{m}\right)}$$

$$\Psi\left[\frac{\lambda_0^+}{2B}\frac{\left(\bar{m}_0 - \frac{2B}{\lambda_0^+}\bar{n}_0\right)\left(m - \frac{2B}{\lambda_0^+}n\right)}{\left(\bar{m} - \frac{2B}{\lambda_0^+}\bar{n}\right)}, \frac{\left(\bar{n} + \frac{\tilde{A}}{\lambda_0^+}\bar{m}\right)\left(n + \frac{\tilde{A}}{\lambda_0^+}m\right)}{\left(\bar{n} + \frac{\tilde{A}}{\lambda_0^+}\bar{m}\right)}\right], \tag{4.9}$$

where Ψ is an arbitrary function. The new non-KNO scaling law that we get for this probability distribution is (dropping constants $\bar{m}_0$ and $\bar{n}_0$) [27]

$$\left(\bar{m} - \frac{2B}{\lambda_0^+}\bar{n}\right)\left(\bar{n} + \frac{\tilde{A}}{\lambda_0^+}\bar{m}\right)P(m, n) = \Psi\left[\frac{m - \frac{2B}{\lambda_0^+}}{\left(\bar{m} - \frac{2B}{\lambda_0^+}\bar{n}\right)}, \frac{n + \frac{\tilde{A}}{\lambda_0^+}}{\left(\bar{n} + \frac{\tilde{A}}{\lambda_0^+}\bar{m}\right)}\right]. \tag{4.10}$$

We see from the first line that Eq. (4.9) has the KNO scaling limit of Eq. (1.1) when $\tilde{A}$ and B are set to zero, in which case $m = \bar{m} = \bar{m}_0$.

We do not have an exact expression for Ψ in Eq. (4.9). We can however define the generating function $G(x, y, t)$,

$$G(x, y, t) = \sum_{m,n} x^m y^n P_{mn}(t). \tag{4.11}$$

Equation (4.3) for $P_{mn}(t)$ gives the evolution equation for G,

$$\frac{\partial G}{\partial t} = -(A+B)\frac{\partial G}{\partial y} + \tilde{A}x\frac{\partial G}{\partial x} + \tilde{A}xy\frac{\partial G}{\partial x} + Ay^2\frac{\partial G}{\partial y} + Bx^2\frac{\partial G}{\partial y} \tag{4.12}$$

which can be solved analytically only in the special case when $A = 2\tilde{A}$ [28]. The explicit form of G is determined by the initial conditions. For the two cases $m_0 = 0$ or $n_0 = 0$ we impose the initial conditions $G(x, y, 0) = y^{n_0}$ or x^{m_0}, respectively. With these two different initial conditions,

$$G_{m_0=0,n_0}(x, y, t) = [1 + (y/x^2 - 1)e^{-Bt}]^{n_0}$$
$$[1 + (1/x^2 - b/(A+B) - Ay/(A+B)x^2)e^{At} + A/(A+B)(y/x^2 - 1)e^{-Bt}]^{-n_0}, \tag{4.13}$$

or

$$G_{m_0,n_0=0}(x, y, t) = \left[1 + \left(\frac{1}{x^2} - \frac{B}{A+B} - \frac{Ay}{A+Bx^2}\right)e^{At} + \frac{A}{A+B}\left(\frac{y}{x^2} - 1\right)e^{-Bt}\right]^{-m_0/2}. \tag{4.14}$$

In Ref. [28] Giovannini obtained these for $n_0 = 1$ and $m_0 = 1$. Even in this special case, Eq. (4.14) is intractable for extracting $P_{mn}(t)$. However, the generating function can be used to obtain moments of P_{mn}, which are the quantities usually obtained experimentally. The x or y derivatives of $G(x, y, t)$ at $x = 1$, $y = 1$ give the moments

$$K_r = \left.\frac{\partial^r G(x, y, t)}{\partial x^r}\right|_{x=1, y=1} = \overline{m(m-1)\ldots(m-r+1)},$$

$$K_s = \left.\frac{\partial^s G(x, y, t)}{\partial y^s}\right|_{y=1, x=1} = \overline{n(n-1)\ldots(n-s+1)}. \tag{4.15}$$

When $A \neq 2\tilde{A}$, so that the explicit form of $G(x, y, t)$ is not known, Eq. (4.12) gives differential equations, the same as Eqs (4.6), for $\bar{m}$ and $\bar{n}$; but equations for higher moments are too complicated.

4.2.2. The decoupled gluon equation

From Eq. (4.8) we see that $\bar{m}/\bar{n} \to 2B/A$ for high energy. We also know that $B \ll A$, that is, pair production is suppressed. Therefore $P_{mn} \to P_n$, which implies that it is a fairly reasonable approximation to count only gluons and neglect those which come from pair produced quarks. We look at this simplified case to investigate further the approach to KNO scaling. With m fixed, Eq. (4.3) becomes

$$\frac{\partial P_n}{\partial t} = -AnP_n - BnP_n - \tilde{A}mP_n + A(n-1)P_{n-1} + B(n+1)P_{n+1} + \tilde{A}mP_{n-1} \tag{4.16}$$

which by Taylor series expansion can be put in the form

$$\frac{\partial P}{\partial t} = -a_0 P - a_0 n\frac{\partial P}{\partial n} + (a_1 - \tilde{A}m)\frac{\partial P}{\partial n} + \frac{a_1}{2}n\frac{\partial^2 P}{\partial n^2} - \frac{a_2}{2}\frac{\partial^2 P}{\partial n^2} + \ldots, \tag{4.17}$$

where

$$a_0 = A - B, \quad a_1 = A + B, \quad a_2 = A - B - \tilde{A}m. \tag{4.18}$$

The a_2 term is smaller by $1/n$ and can be neglected. We define new variables in Eq. (4.17),

$$a = 1 - \frac{\lambda}{a_0}, \quad c = \frac{(a_1 - \tilde{A}m)}{(a_1/2)}, \quad y = \frac{a_0}{(a_1/2)}n \tag{4.19}$$

and find the solution

$$P(n, t) = \int_0^\infty d\lambda w(\lambda) e^{-\lambda_0 t}\Psi(a, c, y). \tag{4.20}$$

Here $\Psi(a, c, y)$ is the confluent hypergeometric function regular for large y, and $w(\lambda_0)$ is an unspecified weight function. For large y,

$$P(n, t)_{y\text{large}} \approx \int_0^\infty d\lambda w(\lambda) e^{-\lambda t}\left[1 - \frac{a(a-c+1)}{y}\right] y^{-a}. \tag{4.21}$$

The first term in the integrand is a KNO scaling piece and the second term is a nonscaling piece suppressed by $1/y \sim 1/n$. The first term scales by the following argument. If we can show that

$$nP(n, t) = f(ne^{-a_0 t}), \tag{4.22}$$

where f is an arbitrary function, then

$$P(n, t) = e^{-a_0 t} g(ne^{-a_0 t}), \tag{4.23}$$

where $g = f/ne^{-a_0 t}$. The mean multiplicity is

$$\bar{n}(t) = \int_0^\infty dn g(ne^{-a_0 t}) = \bar{N}_0 e^{a_0 t}, \tag{4.24}$$

where the constant $\bar{N}_0$ is the integral $\int_0^\infty dx x g(x)$. Combining Eqs (4.23) and (4.24) we have

$$\bar{n}(t)P(n, t) = \bar{N}_0 g\left(\bar{N}_0 \frac{n}{\bar{n}}\right) \tag{4.25}$$

which is the condition for KNO scaling. What remains is to show that the first term in the large y expression for $P(n, t)$ in Eq. (4.21) satisfies Eq. (4.22). The definitions of y and a in Eq. (4.19) lead to

$$nP(n, t) = \frac{a_1}{2a_0} \int_0^\infty d\lambda \omega(\lambda) \left(\frac{2a_0}{a_1} ne^{-a_0 t}\right)^{\lambda/a_0}, \tag{4.26}$$

so the right side of this equation is a function of $ne^{-a_0 t}$, and the dominant part of $P(n, t)$ scales. The nonscaling term in Eq. (4.21) is

$$\begin{aligned} &- \int_0^\infty d\lambda w(\lambda) e^{\lambda t} \frac{a(a-c+1)}{y} y^{-a} \\ &= - \int_0^\infty d\lambda w(\lambda) e^{-\lambda t} \left[\left(\frac{\lambda}{a_0} - 1\right)\left(\frac{\lambda}{q_0} - \frac{2\tilde{A}m}{a_1}\right)\right]^{\lambda_0/a_0 - 1} \\ &= - \int_0^\infty d\lambda_0 w(\lambda_0) e^{-\lambda_0 t} \left[y \frac{d^2}{dy^2} + \left(\frac{a_1 - \tilde{A}m}{a_1/2}\right)\right]^{\lambda_0/a_0 - 1}. \end{aligned} \tag{4.27}$$

Since $y = \dfrac{2a_0 n}{a_1}$, the left side tells us the nonscaling piece falls off as $1/n$. The $e^{-\lambda_0 t}$ in the integrand suppresses the large λ_0 contribution to the integral. Although there is an overall minus sign, the quantity in square brackets on the right side may not always be positive, since it contains λ_0, which ranges from 0 on up. In the range $0 \leqslant \lambda_0 \leqslant a_0$ it can

be shown that the quantity in square brackets ranges from $2\tilde{A}m/a_1$ to 0, always positive when we insert known values of A, $\tilde{A}$, B and assume $m \geqslant 1$. ($\tilde{A}/A = 4/9$ is a standard leading logarithmic value.) When $\lambda_0 \geqslant a_0$, the quantity is positive if $\tilde{A} < a_1/2$. This limit is only safe when $m = 1$, but then for larger λ_0 the condition on $\tilde{A}m$ is relaxed, plus $e^{-\lambda_0 t}$ takes over. The KNO limit is thus approached from below for nearly all values of λ_0 in the integral, and for all values if $m = 1$. For high z, say $z > 2$ or 3, the condition on m can be relaxed and KNO is approached from below for all values of λ_0.

4.2.3. The exact analytic solution of the decoupled quark-gluon equation

In the limit when the quark evolution is neglected we obtain the *exact analytic* expression for the probability distribution, multiplicities and moments [26]. In our parton branching model we assume that hadron-hadron collision takes place in three steps. In step one, partons from hadrons collide. (Their collisions are assumed to be $2 \to 2$ processes.) There are total of m_0 quarks and n_0 gluons involved in collision (since m_0 and n_0 are the average initial numbers of quarks and gluons involved in the collision, m_0 and n_0 need not be integers). After the collision, in step two, these quarks and gluons branch and loose their energy. Finally, in step three, they hadronize. The schematic parton branching model representation of hadron-hadron collision is shown in Fig. 6 [30]. Here we consider steps 1 and 2 and, as usual, we assume that the hadronization process does not alter the main features of the hard process. Due to the fact that as the energy increases the activity of gluons inside hadrons increases and the contribution from gluons to the cross section and multiplicities increases with energy [29], we assume that n_0 increases slowly with energy while m_0 decreases with energy. Therefore at some asymptotic energies only gluon-gluon collision will contribute to the multiplicities. The probability distribution at these energies will be pure gluon branching distribution [30]. This implies that the widening of the distribution and increases of the multiplicity moments have upper bound [31].

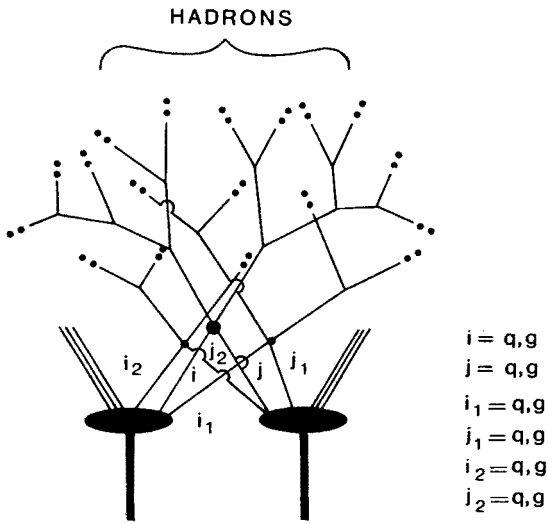

Fig. 6. The schematic parton branching model picture of hadron-hadron collision

As noted before at high energies $\frac{m}{\bar{n}} \sim \frac{\lambda B}{A} \ll 1$ and we can neglect quark evolution ($m = \bar{m} = m_0 = \text{const}$). The evolution equation (4.3) then becomes the evolution equation for the probability P_n

$$\frac{\partial P_n(t)}{\partial t} = -AnP_n + A(n-1)P_{n-1} - BnP_n + B(n+1)P_{n+1} + \tilde{A}m_0 P_{n-1} - \tilde{A}m_0 P_n. \quad (4.28)$$

Assuming n_0 initial gluons and m_0 initial quarks we get the following probability distribution

$$P_n(t) = \left[1 + \frac{A}{(A-B)}(e^{(A-B)t} - 1)\right]^{-n-n_0-k} [e^{(A-B)t} - 1]^{n_0+n} \frac{B^{n_0}A^n}{(A-B)^{n_0+n}}$$

$$\frac{(n+n_0+k-1)!}{n!(n_0+k-1)!} {}_2F_1(-n, -n_0; -n_0-k+1, u), \quad (4.29)$$

where

$$k = \frac{\tilde{A}m_0}{A}$$

and

$$u = 1 - \frac{(A-B)^2 e^{(A-B)t}}{AB(e^{(A-B)t} - 1)^2}. \quad (4.30)$$

It has been shown that this distribution approaches exact KNO scaling in the large n and $\bar{n}$ limit *only* in the case when n_0 and m_0 are energy independent [25]. By rewriting Eq. (4.28) in terms of the generating function defined as $G(y, t) = \Sigma y^n P_n(t)$ we can solve this equation with the initial condition $G(y, 0) = y^{n_0}$. The solution is

$$G(y, t) = \left[1 - \frac{A}{(A-B)}(e^{(A-B)t} - 1)(y-1)\right]^k \left[1 + \frac{e^{(A-B)t}(y-1)}{1 - \frac{A}{(A+B)}(e^{(A-B)t} - 1)(y-1)}\right]^{n_0}. \quad (4.31)$$

Clearly, the multiplicity $\bar{n}$ and moments C_q can be obtained by taking the q-th derivative of the generating function and setting $y = 0$. We get

$$\bar{n} = k\frac{A}{(A-B)}(e^{(A-B)t} - 1) + n_0 e^{(A-B)t}, \quad (4.32)$$

$$C_2 = 1 + \frac{\beta\alpha^2 - n_0(1-\alpha)^2}{\delta^2} + \frac{1}{\bar{n}}\left(1 - \frac{2n_0\alpha\beta}{\delta^2}\right),$$

$$C_3 = 1 + \frac{3[\beta\alpha^2 - n_0(1-\alpha)^2]}{\delta^2} + \frac{2[\alpha^3\beta + n_0(1-\alpha)^3]}{\delta^3}$$

$$+\frac{1}{\bar{n}}\left[3+\frac{\beta\alpha(3\alpha-6n_0)-3n_0(1-\alpha)^2}{\delta^2}+\frac{6n_0\alpha\beta(1-2\alpha)}{\delta^3}\right]$$

$$+\frac{1}{\bar{n}^2}\left[1-\frac{3\alpha n_0\beta(2+\alpha 2k)}{\delta^2}+\frac{6\alpha^2\beta n_0[n_0\alpha+(1-\alpha)\beta]}{\delta^3}\right]$$

$$+\frac{1}{\bar{n}^3}\left[\frac{-3\alpha^2 k n_0\beta}{\delta^2}+\frac{2n_0\alpha^3\beta(\beta^2-n_0^2)}{\delta^3}\right],$$

$$C_4=1+\frac{6[\alpha^2\beta-n_0(1-\alpha)^2]}{\delta^2}+\frac{8[\alpha^3\beta+n_0(1-\alpha)^3]}{\delta^3}$$

$$+\frac{3[n_0(1-\alpha)^4(n_0-2)+\alpha^4\beta(\beta+2)-2\beta n_0(1-\alpha)^2\alpha^2]}{\delta^4}$$

$$+\frac{1}{\bar{n}}\left[6+\frac{18n_0(1-\alpha)^2-12n_0\alpha\beta+18\beta\alpha^2}{\delta^2}\right.$$

$$+\frac{12\alpha\beta[\alpha^2+2n_0(1-\alpha)^2-2n_0\alpha^2]+12n_0(1-\alpha)^3}{\delta^3}$$

$$\left.+\frac{12n_0\beta[n_0\alpha^2(1-\alpha)^2-\beta\alpha^3(1-\alpha)+(n_0-2)(1-\alpha)^3-\alpha^4(\beta+2)]}{\delta^4}\right]$$

$$+\frac{1}{\bar{n}^2}\left[7+\frac{[6n_0\beta\alpha^2(n_0-\beta)+7\beta\alpha^2-7n_0(1-\alpha)^2-36n_0\beta\alpha]}{\delta^2}\right.$$

$$+\frac{[36n_0\alpha\beta(1-2\alpha)+24n_0\alpha^2\beta^2(1-\alpha)+24\alpha^3n_0^2\beta]}{\delta^3}$$

$$+\frac{36n_0\alpha^2\beta[n_0\alpha^2-(1-\alpha)^2\beta]+18n_0^2\alpha^2\beta^2[\alpha^2+(1-\alpha)^2]}{\delta^4}$$

$$\left.+\frac{24n_0^2\alpha^3(1-\alpha)\beta^2-6n_0\alpha^2\beta[n_0^2(1-\alpha)+\alpha^2\beta^2]}{\delta^4}\right]$$

$$+\frac{1}{\bar{n}^3}\left[1-\frac{14n_0\alpha\beta+18n_0\beta\alpha^2(\beta-n_0)}{\delta^2}+\frac{8n_0\alpha^3\beta(\beta^2-n_0^2)+36n_0\alpha^2\beta[(1-\alpha)\beta+n_0\alpha]}{\delta^3}\right.$$

$$\left.+\frac{12n_0^2\alpha^3\beta^2(n_0-\beta)+24n_0\alpha^3\beta[n_0^2-(1-\alpha)\beta]}{\delta^4}\right]$$

$$+\frac{1}{\bar{n}^4}\left[\frac{7n_0\alpha^2\beta(n_0-\beta)}{\delta^2}+\frac{12n_0\alpha^3\beta(\beta^2-n_0^2)}{\delta^3}\right.$$

$$\left.+\frac{6n_0\alpha^4\beta(n_0^3-\beta^3)+3n_0^2\alpha^4\beta^2(n_0^2+\beta^2-2n_0\beta)}{\delta^4}\right], \tag{4.33}$$

where $\alpha = \dfrac{A}{(A-B)}$, $\beta = k+n_0$ and $\delta = k\alpha+n_0$. The analytic expression for C_5 is not displayed because of its length.

We note that the parton branching distribution given by Eq. (4.29) is very similar to the very popular negative binomial distribution. Namely, in the limit when $\alpha = 1$ and $\delta = k$ (or n_0) we get the negative binomial distribution (or simple gluon branching distribution). The probability distribution, multiplicities and moments are given by

$$P_n^{\delta} = \frac{(n-\frac{1}{2}\pm\delta\mp\frac{1}{2})!}{n!(\delta-1)!}\left(\frac{\delta}{\bar{n}}\right)^{\delta}\left(1\pm\frac{\delta}{\bar{n}}\right)^{\mp n-\delta},$$

$$\bar{n} = \delta e^{At} - \frac{\delta}{2}\mp\frac{\delta}{2},$$

$$C_2 = 1+\frac{1}{\delta}\pm\frac{1}{\bar{n}}, \quad C_3 = 1+\frac{3}{\delta}+\frac{2}{\delta^2}\pm\frac{1}{\bar{n}}\left(3+\frac{3}{\delta}\right)+\frac{1}{\bar{n}^2},$$

$$C_4 = 1+\frac{6}{\delta}+\frac{11}{\delta^2}+\frac{6}{\delta^3}\pm\frac{1}{\bar{n}}\left(6+\frac{18}{\delta}+\frac{12}{\delta^2}\right)+\frac{1}{\bar{n}^2}\left(7+\frac{7}{\delta}\right)\pm\frac{1}{\bar{n}^3},$$

$$C_5 = 1+\frac{10}{\delta}+\frac{35}{\delta^2}+\frac{50}{\delta^3}+\frac{24}{\delta^4}\pm\frac{1}{\bar{n}}\left(10+\frac{60}{\delta}+\frac{110}{\delta^2}-\frac{60}{\delta^3}\right)$$
$$+\frac{1}{\bar{n}^2}\left[25+\frac{75}{\delta}+\frac{190}{\delta^2}\right]\pm\frac{1}{\bar{n}^3}\left[15+\frac{15}{\delta}\right]+\frac{1}{\bar{n}^4}\left[1+\frac{50}{\delta}\right].$$

The negative binomial distribution was first proposed by Knox in 1974 [32] and recently considerably improved and extended in many stochastic models [6]. This distribution has been widely used by UA5 Group to fit the experimental data even though in all stochastic models there is *no* physical understanding of the behaviour of the parameter k (which is interpreted as the number of independently emitting sources and it decreases drastically with energy from 20 at $\sqrt{s} = 10$ GeV to 3 at $\sqrt{s} = 900$ GeV). In our model, k is related to the average number of initial quarks and for the Collider energies (200 GeV $\leqslant \sqrt{s} \leqslant$ 900 GeV) it decreases from 3 to 0.9 while the average number of initial gluons n_0 increases from 1.3 to 2 in the same energy range. We also give theoretical predictions for the values of the parameter k at Tevatron Collider energies.

Assuming that the average initial number of gluons n_0 increases slowly with energy while the average initial number of quarks m_0 decreases, we fit the data for the multiplicity moments C_2, C_3, C_4 and C_5 in the energy range 30.4 GeV $\leqslant \sqrt{s} \leqslant$ 900 GeV (Table I and Fig. 7). Since $B \gg A$ at high energies, the parameter α decreases with energy approaching 1 at $\sqrt{s} = 900$ GeV. The fact that initial number of quarks is large at low energy ($\sqrt{s} \sim 30$ GeV) indicates that our approximation of neglecting the quark evolution is not good at these energies. We need to consider the probability distribution P_{mn} which is a solution of the evolution equation (4.3). However for the high enough energies ($\sqrt{s} \sim 200$ GeV,

TABLE I

Theoretical predictions for the moments C_2, C_3, C_4 and C_5 for the energy range $30.4 \leqslant \sqrt{s} \leqslant 900$ GeV [26] compared with their experimental values given in the brackets. Parameters k and n_0 are fitted with $k \sim 11.4\text{–}1.51 \ln \sqrt{s}$ and $n_0 \sim -0.007 + 0.295 \ln \sqrt{s}$. Theoretical predictions for the multiplicities and moments for Tevatron Collider energies ($\sqrt{s} \sim 1600$ GeV, $\sqrt{s} \sim 1800$ GeV and $\sqrt{s} \sim 2000$ GeV) indicate the upper bounds for the moments C_q. The error bars in the predictions for the moments C_q at Tevatron Collider energies are due to the uncertainty in extrapolation of the energy dependence of the parameters k and n_0

$\sqrt{s}$ (GeV)	k	n_0	α	$\bar{n}$	C_2	C_3	C_4	C_5
30.4	6	1	1.1	10.3 (10.07 ± 0.1)	1.22 (1.21 ± 0.01)	1.68 (1.70 ± 0.02)	2.72 (2.64 ± 0.1)	4.60 (4.6 ± 0.3)
62.6	5	1.2	1.09	13.9 (13.6 ± 0.1)	1.21 (1.20 ± 0.01)	1.68 (1.65 ± 0.02)	2.71 (2.60 ± 0.08)	4.49 (4.4 ± 0.2)
200	3	1.3	1.05	21.1 (21.6 ± 0.5)	1.26 (1.26 ± 0.03)	1.89 (1.91 ± 0.12)	3.33 (3.3 ± 0.03)	6.13 (6.6 ± 0.9)
540	$1.5\dot{5}$	1.6	1.03	28.8 (28.3 ± 0.2)	1.32 (1.31 ± 0.03)	2.19 (2.12 ± 0.11)	4.23 (4.05 ± 0.32)	8.50 (8.8 ± 1.0)
900	0.9	2	1	33.2 (35.1 ± 0.6)	1.33 (1.34 ± 0.03)	2.24 (2.22 ± 0.13)	4.46 (4.3 ± 0.4)	9.28 (9.3 ± 1.1)
1600	0	2.06 ± 0.11	1	38.6	1.46 ± 0.02	2.85 ± 0.13	6.79 ± 0.52	17.22 ± 1.95
1800	0	2.09 ± 0.11	1	39.78	1.45 ± 0.02	2.82 ± 0.13	6.67 ± 0.52	16.77 ± 1.93
2000	0	2.11 ± 0.11	1	40.84	1.45 ± 0.02	2.81 ± 0.12	6.59 ± 0.49	16.44 ± 1.79

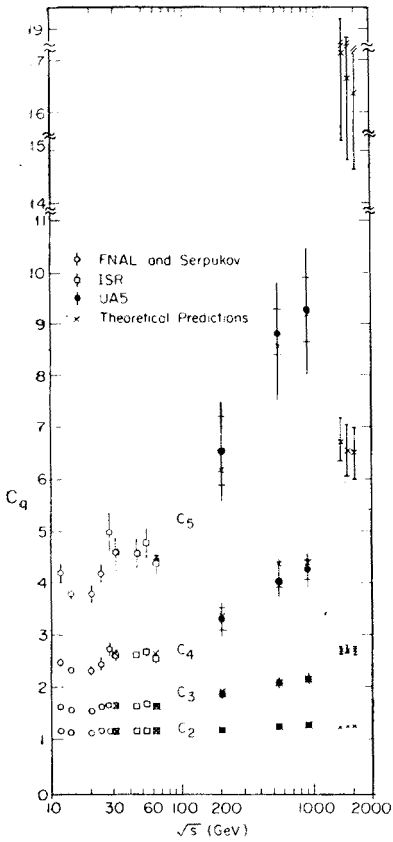

Fig. 7. The theoretical predictions for the moments C_2, C_3, C_4 and C_5 plotted as a function of energy and compared with the experimental data in the energy range 10 GeV $\leqslant \sqrt{s} \leqslant$ 900 GeV. Theoretical prediction for the moments C_q for the Tevatron Collider energies is included

$k = 3$, $m_0 = 6$) we can safely neglect quark evolution and our distribution describes the data remarkably well. The values for $\bar{n}$ in Table I are taken from the experimental fit [2] ($\bar{n} \sim 2.7 - 0.03 \ln s + 0.167 \ln^2 s$). In order to satisfy our assumption that k decreases with energy while n_0 increases with energy we find that the best fits for the moments C_2 are obtained with $k \sim 11.4 - 1.51 \ln \sqrt{s}$ and $n_0 \sim -0.007 + 0.295 \ln \sqrt{s}$. The values for the moments C_3, C_4 and C_5 are calculated with these values of k and n_0. Extrapolating the energy dependence of parameters k and n_0 (Fig. 8), we predict that at $\sqrt{s} \sim 1700$ GeV ± 100 GeV (the solid line in Fig. 8 corresponds to $\sqrt{s} \sim 1600$ GeV, while the dashed line corresponds to $\sqrt{s} \sim 1800$ GeV) the average number of initial quarks is zero and the widening of the distribution stops.

This gives the following upper bounds on moments C_q:

$$C_{2\max} \leqslant 1.46 \pm 0.02, \quad C_{3\max} \leqslant 2.85 \pm 0.13,$$

$$C_{4\max} \leqslant 6.79 \pm 0.52, \quad C_{5\max} \leqslant 17.22 \pm 1.95. \tag{4.35}$$

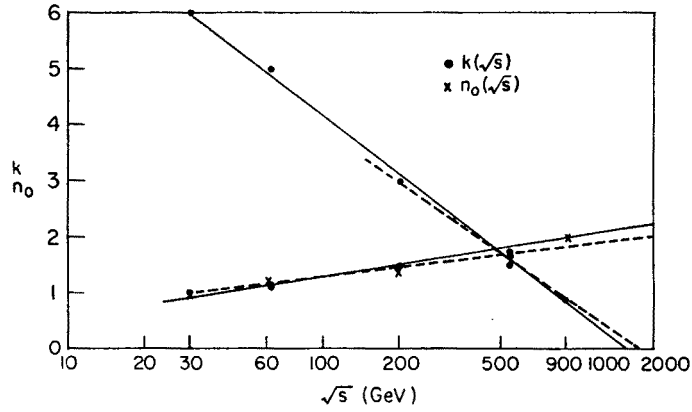

Fig. 8. The theoretical parameters k and n_0 plotted as a function of energy with the assumption that the initial number of gluons increases with energy while the initial number of quarks decreases with energy. Extrapolating values for k and n_0 to higher energies we find that k approaches 0 (m_0 approaches 0) at $\sqrt{s} \sim 1700$ GeV $\pm$ 100 GeV (the solid line corresponds to $\sqrt{s} \sim 1600$ GeV, while the dashed line corresponds to $\sqrt{s} \sim 1800$ GeV). This implies that at this energy the probability distribution reaches its maximum width. It also sets the upper limits on the moments C_q

The upper (lower) limit of the $C_{q\,\max}$ is determined using the extrapolation of $k(\sqrt{s})$ given by the solid (dashed) line and the extrapolation of n_0 given by the dashed (solid) line in Fig. 8. The theoretical uncertainty in these predictions is comparable with the experimental uncertainty in the measurements of the moments C_q in this energy range. From Table I we see that the experimental uncertainty is larger for the higher moments and higher energies.

As energy increases from $\sqrt{s} \sim 1700$ GeV $\pm$ 100 GeV up the contribution to the multiplicities is only coming from gluons. The probability distribution is the pure gluon branching distribution given by Eq. (4.34). The initial number of gluons n_0 will continue to increase resulting in the narrowing of the probability distribution which is in agreement with other QCD based approaches to KNO scaling problem in hadron-hadron collisions [33]. We differ from other QCD based models in considering the evolution of *both* quarks *and* gluons. At $\sqrt{s} \sim 200$ GeV we can neglect quark evolution, but gluons are still produced from quarks by quark bremsstrahlung as well as from gluons by gluon branching. This results in widening of the probability distribution up to Tevatron Collider energies which is in agreement with the experimental data. Ones the contribution to the multiplicities is coming only from the gluons (at Tevatron energies), the probability distribution starts narrowing. We give predictions for the multiplicities and moments C_q for the Tevatron Collider energies [26] ($\sqrt{s} \sim 1600$ GeV, $\sqrt{s} \sim 1800$ GeV, $\sqrt{s} \sim 2000$ GeV in Table I and Fig. 7) indicating the slow narrowing of the probability distribution in this energy range. We also predict the values for the parameters k and n_0 for the Tevatron Collider energies [31].

I am very grateful to the organizers of the XXVII Kraków School of Theoretical Physics, especially A. Białas, W. Czyż and W. Słomiński for their hospitality. I would like to thank my collaborators P. Carruthers and B. Durand for many useful discussions.

Part of this work was motivated by discussion with T. Goldman and S. Raby who I also thank for many interesting suggestions. I am also indebted to F. Cooper, R. Hughes, J. Lykken, Ta-Chung Meng and G. West for helpful comments.

REFERENCES

[1] For review see P. Carruthers, C. C. Shih, *International Journal of Modern Physics* **A2**, 1447 (1987).
[2] Z. Koba, H. B. Nielsen, P. Olesen, *Nucl. Phys.* **B40**, 317 (1972).
[3] W. Tome et al., *Nucl. Phys.* **B129**, 365 (1972); J. Firestone et al., *Phys. Rev.* **D14**, 2902 (1976).
[4] UA5 Collaboration, G. J. Alner et al., *Phys. Lett.* **138B**, 304 (1984); **160B**, 193 (1985).
[5] UA5 Collaboration, G. J. Alner et al., *Phys. Lett.* **160B**, 199 (1985).
[6] P. Carruthers, C. C. Shih, *Phys. Lett.* **127B**, 242 (1983); **137B**, 425 (1984); M. Biyajima, *Prog. Theor. Phys.* **69**, 966 (1983); A. Giovannini, L. Van Hove, CERN-TH-4330/85; R. Weiner, Proc. Local Equilibrium, Singapore 1986.
[7] UA5 Collaboration, G. J. Alner et al., CERN-EP/85-62.
[8] UA1 Collaboraton, G. Ciapetti, in Proceedings of the Fifth Topical Workshop on Proton-Antiproton Collider Physics, St. Vincent Aosta Valley, Italy 1985, ed. by M. Greco, World Scientific, Singapore 1985, p. 488; UA1 Collaboration, F. Ceradini et al., CERN Report No. CERN-EP-85-196, to be published.
[9] P. Aurenche, F. W. Bopp, *Z. Phys.* **C13**, 459 (1982); A. Capella, J. Tran Thanh Van, *Z. Phys.* **C23**, 165 (1984).
[10] A. Capella, J. Kwieciński, J. Tran Than Van, *Phys. Rev. Lett.* **58**, 2015 (1987).
[11] T. T. Chou, C. N. Yang, *Phys. Rev.* **D32**, 1692 (1985).
[12] T. T. Chou, C. N. Yang, *Phys. Lett.* **54**, 510 (1985).
[13] Cau Xu, Liu Lian-sou, *Lett. Nuovo Cimento* **37**, 495 (1983); Cai Xu, Chao Wei-quin, Meng Ta-chung, *Phys. Rev.* **D33**, 1287 (1986).
[14] F. Hayot, H. Navelet, *Phys. Rev.* **D30**, 2322 (1984).
[15] G. Pancheri, Y. N. Srivastava, M. Palota, *Phys. Lett.* **151B**, 453 (1985).
[16] T. K. Gaisser, F. Halzen, A. D. Martin, C. J. Maxwell, *Phys. Lett.* **166B**, 219 (1986); S. Rudaz, P. Valin, *Phys. Rev.* **D34**, 2025 (1986).
[17] P. Carruthers, Proceedings of the XV Multiparticle Dynamics Symposium, Lund, Sweden, June 1984.
[18] P. Carruthers, Invited paper presented at Conference on Physics of the 21st Century, Tucson, Arizona, December 1983.
[19] A. Giovannini, L. Van Hove, CERN-TH 4330/85.
[20] P. Carruthers, I. Sarcevic, *Phys. Lett.* **189B**, 442 (1987).
[21] P. Carruthers, I. Sarcevic, LA-UR-87-2396, to be published in *Review Volume on Multiparticle Production*, World Scientific, May 1988.
[22] P. Carruthers, in the Proceedings of the First International Workshop on Local Equilibrium in Strong Interaction Physics, eds D. Scott, R. Weiner, World Scientific 1985.
[23] M. Biyajima, *Phys. Lett.* **137B**, 225 (1984); M. Biyajima, N. Suzuki, *Phys. Lett.* **143B**, 463 (1984).
[24] P. Carruthers, F. Zachariasen, *Phys. Rev.* **D13**, 950 (1976); *Rev. Mod. Phys.* **55**, 245 (1983).
[25] B. Durand, I. Sarcevic, *Phys. Lett.* **172B**, 104 (1986); I. Sarcevic, in Proceedings of the XVII International Symposium on Multiparticle Dynamics, eds M. Markytan, W. Majerotto, J. MacNaughton, p. 639, World Scientific 1987; I. Sarcevic, in Proceedings of the Second International Workshop on Local Equilibrium in Strong Interaction Physics, eds P. Carruthers, D. Strottman, p. 160, World Scientific 1986.
[26] I. Sarcevic, *Phys. Rev. Lett.* **59**, 403 (1987).
[27] B. Durand, I. Sarcevic, *Phys. Rev.* **D36**, 2693 (1987).
[28] A. Giovannini, *Il Nuovo Cimento* **A15**, 543 (1973); *Nucl. Phys.* **B161**, 429 (1979).

[29] E. Eichten, I. Hinchliffe, K. Lane, C. Quigg, *Rev. Mod. Phys.* **56**, 579 (1984); T. K. Gaisser, F. Halzen, *Phys. Rev. Lett.* **54**, 1754 (1985); G. Pancheri, Y. Srivastava, M. Palota, *Phys. Lett.* **151B**, 453 (1985); S. Rudaz, P. Valin, *Phys. Rev.* **D34**, 2025 (1986).

[30] S. Ellis, Proceedings of the XIth SLAC Summer Institute, SLAC Report 267 (1983); B. Durand, S. D. Ellis, Proceedings of 1984 Summer Study on the Design and Utilization of the SSC, Snowmass, CO 1984.

[31] I. Sarcevic, *Mod. Phys. Lett.* **A2**, 513 (1987).

[32] W. Knox, *Phys. Rev.* **D10**, 65 (1974).

[33] F. Hayot, G. Sterman, *Phys. Lett.* **121B**, 419 (1983); G. Pancheri, Y. N. Srivastava, *Phys. Lett.* **128B**, 433 (1983); F. Hayot, H. Navelet, *Phys. Rev.* **D30**, 2322 (1984).